ARTICLE

Multicomponent Solubility Parameters for Single-Walled Carbon Nanotube–Solvent Mixtures

Shane D. Bergin,[†] Zhenyu Sun,[†] David Rickard,[†] Philip V. Streich,[‡] James P. Hamilton,[‡] and Jonathan N. Coleman[†,§,*]

[†]School of Physics, Trinity College Dublin, Dublin 2, Ireland, [‡]Department of Chemistry and Engineering Physics, University of Wisconsin—Platteville, Platteville, Wisconsin 53818, and [§]Centre for Research on Adaptive Nanostructures and Nanodevices (CRANN), Trinity College Dublin, Dublin 2, Ireland

ABSTRACT We have measured the dispersibility of single-walled carbon nanotubes in a range of solvents, observing values as high as 3.5 mg/mL. By plotting the nanotube dispersibility as a function of the Hansen solubility parameters of the solvents, we have confirmed that successful solvents occupy a well-defined range of Hansen parameter space. The level of dispersibility is more sensitive to the dispersive Hansen parameter than the polar or H-bonding Hansen parameter. We estimate the dispersion, polar, and hydrogen bonding Hansen parameter for the nanotubes to be $<\delta_D> = 17.8$ MPa$^{1/2}$, $<\delta_P> = 7.5$ MPa$^{1/2}$, and $<\delta_H> = 7.6$ MPa$^{1/2}$. We find that the nanotube dispersibility in good solvents decays smoothly with the distance in Hansen space from solvent to nanotube solubility parameters. Finally, we propose that neither Hildebrand nor Hansen solubility parameters are fundamental quantities when it comes to nanotube–solvent interactions. We show that the previously calculated dependence of nanotube Hildebrand parameter on nanotube diameter can be reproduced by deriving a simple expression based on the nanotube surface energy. We show that solubility parameters based on surface energy give equivalent results to Hansen solubility parameters. However, we note that, contrary to solubility theory, a number of nonsolvents for nanotubes have both Hansen and surface energy solubility parameters similar to those calculated for nanotubes. The nature of the distinction between solvents and nonsolvents remains to be fully understood.

KEYWORDS: nanotube · solvent · solubility parameters

*Address correspondence to colemaj@tcd.ie.

Received for review May 13, 2009 and accepted July 27, 2009.

Published online August 5, 2009.
10.1021/nn900493u CCC: $40.75

Carbon nanotubes are among the most exciting of nanomaterials due to their superlative physical properties.[1] However, nanotubes are generally produced as an intractable black powder that must be exfoliated before use. Exfoliation is usually carried out in the liquid phase and is the starting point for many processing or preparation procedures. In fact, a very wide range of techniques, from composite formation[2] to spectroscopic characterization,[3] are heavily reliant on liquid phase exfoliation of nanotubes. The most common exfoliation method is to disperse the nanotubes as a colloidal suspension, usually stabilized with the aid of surfactants,[4,5] polymers,[6,7] or DNA.[8,9] However, for both practical and aesthetic reasons, it would be preferable to disperse nanotubes using only solvents without the need for any third phase dispersant.

In recent years, a number of papers have appeared describing the preparation of stable suspensions of single-walled nanotubes (SWNTs) in a range of common solvents.[10−18] This work originated in 2001 when Bahr *et al.* demonstrated dispersion of nanotubes in various solvents.[11] As time has gone on, it has become increasingly clear that nanotubes can be suspended and even exfoliated in a range of solvents up to concentrations as high as 0.125 mg/mL.[19] Both for the purposes of basic research and in order to improve nanotube dispersion, it is of great interest to attempt to understand the dispersion process. In this paper, we do just that by correlating the dispersibility of SWNTs in various solvents with both Hildebrand and Hansen solubility parameters. In addition, we propose a new set of solubility parameters which may be more appropriate for nanomaterials such as nanotubes or graphene.

THEORETICAL BACKGROUND

First, we must briefly review solubility theory in its simplest form. In general, a substance is said to be soluble in a given solvent if the free energy of mixing, ΔG_{mix}, for the solute–solvent mixture is negative. The free energy of mixing has both enthalpic and entropic components such that

$$\Delta G_{mix} = \Delta H_{mix} - T\Delta S_{mix} \quad (1)$$

where ΔH_{mix} and ΔS_{mix} are the enthalpy and entropy of mixing, respectively, and T is the absolute temperature. This means that a solution is defined by $\Delta H_{mix} < T\Delta S_{mix}$. If this is not the case (*i.e.*, if $\Delta H_{mix} > T\Delta S_{mix}$), we have a suspension or a dispersion. In

general, ΔS_{mix} is a measure of the increased disorder associated with the mixture compared with the individual pure components. As such, ΔS_{mix} is always positive and is calculated on a statistical basis.[20−22] For a flexible polymer in a liquid, it is given by[22]

$$\Delta \bar{S}_{mix} = -\frac{k}{v_0}\left[(1-\phi)\ln(1-\phi) + \frac{\phi}{x}\ln\phi\right] \quad (2)$$

Here, $\Delta \bar{S}_{mix}$ is the entropy of mixing per volume of mixture, ϕ is the solute volume fraction, v_0 is the solvent molecular volume (lattice site volume in the lattice theory), while x is the degree of polymerization.

In contrast, ΔH_{mix} is a measure of the energetic cost of separating the individual solvent and solute molecules less the energy gain from surrounding the solute molecules by solvent molecules. Thus, depending on the system, ΔH_{mix} can be either negative or positive but is usually positive.

For mixtures of small molecules, ΔH_{mix} is usually expressed in terms of either the Flory−Huggins expression:[21,22]

$$\Delta \bar{H}_{mix} = \chi\phi(1-\phi)kT/v_0 \quad (3)$$

or the Hildebrand−Scratchard expression:[21,22]

$$\Delta \bar{H}_{mix} \approx (\delta_{T,A} - \delta_{T,B})^2\phi(1-\phi) \quad (4)$$

Here, $\Delta \bar{H}_{mix}$ is the enthalpy of mixing per volume of mixture, χ is the Flory−Huggins parameter, and $\delta_{T,A}$ and $\delta_{T,B}$ are the Hildebrand solubility parameters of the solute and solvent, respectively. We note that eq 3 is approximate. Use of the geometric mean approximation in the derivation results in the spurious prediction of only positive values of $\Delta \bar{H}_{mix}$. The solubility parameter of a material is easily found as it is just the square root of the (total) cohesive energy density ($E_{C,T}/V$) of the material: $\delta_T = \sqrt{E_{C,T}/V}$. It is clear that χ is related to $\delta_{T,A}$ and $\delta_{T,B}$ by

$$\chi \approx \frac{v_0}{kT}(\delta_{T,A} - \delta_{T,B})^2 \quad (5)$$

Thus, solubility is completely determined by the magnitude and sign of χ which is related to $\delta_{T,A}$ and $\delta_{T,B}$. For most systems, χ is positive, resulting in a positive value of ΔH_{mix}. As a result, most solutions are driven by a large positive value of ΔS_{mix}.

However, carbon nanotubes are certainly not small molecules, and so this basic theory needs some modification. They are best modeled as rigid rods and so can be described by Flory's theory.[23] This predicts that, while rigid rods can form isotropic solutions at low concentration, they form into a nematic phase at higher concentrations. For the current purposes, the main difference between the model described above and Flory's theory is the entropy of mixing. For an isotropic solution of rigid rods, the absolute entropy of mixing (calculated by comparison with a starting crystalline array of rods) is given by[20,24]

$$\Delta S_{mix} = -k\left[n_s\ln(1-\phi) + n_{NT}\ln\frac{\phi}{x} + n_{NT}(x-1)\right] \quad (6)$$

where n_s and n_{NT} are the numbers of solvent molecules and rods, respectively. Similar to before, x is the rod aspect ratio. We can easily rewrite this on a per volume of mixture basis:[17]

$$\Delta \bar{S}_{mix} = -\frac{k}{v_0}\left[(1-\phi)\ln(1-\phi) + \frac{\phi}{v_{NT}/v_0}\left(\ln\left(\frac{\phi}{x}\right) + (x-1)\right)\right] \quad (7)$$

Here v_0 and v_{NT} are the solvent and rod molecular volumes, respectively. This expression can be compared with that for a flexible polymer (eq 2). The presence of the $(x-1)$ term means that rigid rods have much smaller entropy of mixing than flexible polymers. This means that, due to their large size and considerable rigidity, nanotubes have relatively small ΔS_{mix}.[17]

This means that, for nanotubes to be soluble in a given solvent, ΔH_{mix} would have to be small or negative. For this reason, the energetics of the solvent−nanotube interaction are critically important. Only one solvent−nanotube system, SWNTs in NMP, has been shown to have a negative ΔH_{mix}.[17] The vast majority of systems have positive ΔH_{mix} and so are metastable at best. However, some metastable colloidal dispersions are stable for extremely long times, in excess of hundreds of years; for example Faraday's gold sols are still stable today. Indeed, nanotubes form metastable dispersions in a range of solvents which almost certainly have positive ΔH_{mix}.[10,11,13−15] It has been suggested that such systems may be stabilized against aggregation by solvent−nanotube charge transfer.[25] This would result in a stabilization mechanism similar to that found in surfactant-stabilized systems.[26,27] However, without quantification, we cannot assume the level of charge transfer to be sufficient to stabilize the system alone. Thus, we suggest that good quality nanotube−solvent dispersions are characterized by very low enthalpy of mixing. Thus, it would be useful to understand the conditions where ΔH_{mix} is minimized; that is, when is χ small? Or alternatively, when is $\delta_{T,NT} \approx \delta_{T,Sol}$? As the solubility parameters of solvents are well-documented,[28] this reduces to knowledge of the solubility parameter for carbon nanotubes.

In fact, it is well-known that most systems are not well-described by one solubility parameter. The reason for this is that the Hildebrand−Scratchard equation is based on the so-called geometric mean approximation which is really only applicable to compounds which interact solely through London or dispersion interactions.[21] This of course is not the case for the vast majority of systems. Most molecular interactions are a combination of dispersive, polar, and hydrogen

bonding interactions. To account for this, Hansen proposed that the cohesive energy density of any material is just the sum of dispersive, polar, and hydrogen bonding components:[29]

$$\frac{E_{C,T}}{V} = \frac{E_{C,D}}{V} + \frac{E_{C,P}}{V} + \frac{E_{C,H}}{V} \quad (8)$$

This leads to three solubility parameters, each one equal to the square root of the associated cohesive energy density. Thus, the sum of the squares of these Hansen solubility parameters equals the square of the Hildebrand solubility parameter, δ_T:

$$\delta_T^2 = \delta_D^2 + \delta_P^2 + \delta_H^2 \quad (9)$$

where δ_D, δ_P, and δ_H are the dispersive, polar, and hydrogen bonding solubility parameters. Values for the Hansen parameters of many solvents are known in the literature.[29] In addition HSPiP software (www.hansen-solubility.com) contains a database of Hansen parameters for over 1200 solvents. Within this new scheme, we can write the Flory−Huggins parameter as[29]

$$\chi \approx \frac{v_0}{kT}[(\delta_{D,A} - \delta_{D,B})^2 + (\delta_{P,A} - \delta_{P,B})^2 + (\delta_{H,A} - \delta_{H,B})^2] \quad (10)$$

We note that the second and third terms on the right-hand side of eq 7 have been modified by Hansen with a prefactor of 0.25.[29] While such a factor has been used in Prigogine's theory,[30] we find no convincing justification for using it. Thus, we use eq 10 in its simplest form. Equation 10 means that, for a solute/solvent mixture, the enthalpy of mixing is minimized when solute and solvent have similar values for all three Hansen parameters. We note that, like eq 5, eq 10 is of course approximate as it can only output positive values of χ. Some dispersions predicted by eq 10 (or eq 5) to have very small positive values of χ may in fact have negative values of χ.

Thus, it is critical to know the values for the various solubility parameters for carbon nanotubes. Very little work has been done in this area. Usrey *et al.*[31] and Maiti *et al.*[32] have calculated the Hildebrand parameters of nanotubes, while Detriche *et al.*[33] and Ham *et al.*[34] have estimated the Hansen parameters of SWNTs. Since these papers were published, we have discovered a number of new solvents for carbon nanotubes that are superior to any others (J.N. Coleman and J.P. Hamilton, unpublished work). Thus, it is important to use these new solvents to estimate the Hansen parameters for carbon nanotubes. In this paper, we measure the maximum dispersibility of single-walled nanotubes in a range of solvents including a number of previously undisclosed ones. We analyze the data in terms of the Hansen solubility parameters of the solvents. Using the nanotube dispersibility in each solvent as a weighting, we calculate the weighted average of the Hansen parameters for the set of solvents. We propose that this can be used to approximate the Hansen parameters of the nanotubes. In addition, we suggest that the solubility parameters, either Hildebrand or Hansen, are not fundamental quantities for nanotubes. We propose that the surface energy is a more appropriate property which can be used to calculate both the cohesive energy density and the Hildebrand parameter.

RESULTS AND DISCUSSION

The dispersibility of nanotubes was measured in a range of solvents (best 14 shown in Table 1, the rest are shown in Supporting Information), some of which are known to be extremely good at dispersing nanotubes. These solvents were identified in three ways. Some (*i.e.*, NMP,[12,15] DMF[12,13]) were known from the

TABLE 1. SWNT Dispersibility as Defined by Concentration after Centrifugation (with error) for the Solvents Studied in This Work[a]

	C_{max} (mg/mL)	ΔC_{max} (mg/mL)	ST (mJ/m^2)	δ_D (MPa$^{1/2}$)	δ_P (MPa$^{1/2}$)	δ_H (MPa$^{1/2}$)	δ_T (MPa$^{1/2}$)
CHP[b] (cyclohexyl-pyrrolidinone)	3.5	0.4	38.8	18.2	6.8	6.5	20.5
DMPU (dimethyl-tetrahydro-2-pyrimidinone)[c]	0.65	0.12	40.9	17.8	9.5	9.3	22.2
NBP (*N*-butyl-pyrrolidinone)[b]	0.279	0.002	34.5	17.5	9.9	5.8	20.9
NBenP (benzyl-pyrrolidinone)[b]	0.18	0.02	45.0	18.2	6.1	5.6	20.0
NMP (*N*-methyl-pyrrolidinone)[b]	0.116	0.01	40.0	18	12.3	7.2	23.0
OPPN (3-(2-oxo-1-pyrrolidinyl)propanenitrile)[c]	0.115	0.016	47.2	18.1	12.5	7.1	23.1
NEP (*N*-ethyl-pyrrolidinone)[b]	0.101	0.006	36.9	18	12	7	22.7
N8P (*N*-octyl-pyrrolidone)[c]	0.092	0.026	34.5	17.4	6.2	4.8	19.1
NVP (*N*-vinyl-pyrrolidinone)[b]	0.084	0.004	42.7	16.4	9.3	5.9	19.8
DMEU (dimethyl-imidazolidinone)[c]	0.083	0.014	42.5	18.0	10.5	9.7	23.0
DMA (dimethylacetamide)[b]	0.041	0.024	36.7	16.8	11.5	10.2	22.8
NFP (*N*-formyl-piperidine)[c]	0.039	0.012	41.3	18.7	9.6	7.5	22.3
N12P (*N*-dodecyl-pyrrolidone)[c]	0.030	0.008	33.5	17.5	4.1	3.2	18.3
DMF (dimethylformamide)[b]	0.023	0.006	37.1	17.4	13.7	11.3	24.9
weighted average				18.0	7.8	6.9	20.9

[a]Also given is the solvent surface tension, the dispersion, polar, and hydrogen bonding Hansen parameters and the Hildebrand solubility parameter. [b]The Hansen parameters of these solvents were taken from the textbook, Hansen Solubility Parameters.[29] [c]The Hansen parameters of these solvents were calculated using HSPiP software (www.hansen-solubility.com).

literature. Others were identified as close structural relations to NMP. Still others were found by testing solvents with surface energy close to that of SWNTs.[17] In addition, during this work, we made preliminary estimations of the nanotube Hansen parameters, using this information to find new solvents. We note that all of the top 14 solvents shown in Table 1 are amide solvents. Note that all the successful solvents have surface tensions (closely related to surface energy; see ref 17) close to 40 mJ/m^2.

The solvent quality was measured in a range of solvents by preparing dispersions by sonication and using centrifugation to remove undispersed material. In this work, we are using optimized sonication conditions (J.N. Coleman and J.P. Hamilton, unpublished work) and, as such, obtain dispersions with relatively high concentration remaining after centrifugation. This procedure is known to give high-quality dispersions containing only individual nanotubes and small bundles.[18] For example, we have observed NMP,[18] CHP, and NBenP to display bundle sizes of less than 6 nm at reasonably high concentrations (J.N. Coleman and J.P. Hamilton, unpublished work). The concentration after centrifugation was measured by UV−vis−IR absorption spectroscopy. We associate this concentration (see Table 1) with the nanotube dispersibility.

Our best result was for CHP, which displayed a dispersibility of $C_{max} = 3.5 \pm 0.4$ mg/mL. This is a very high concentration on the scale of nanotube−solvent dispersions. As far as the authors are aware, the highest reported SWNT dispersibility is 0.125 mg/mL for DMF dispersions.[19] Similarly, dispersibilities of 0.07 mg/mL for SWNTs in tetrachloroethylene[35] and 0.095 mg/mL for SWNTs in dichlorobenzene[11] have been reported. However, it is critical to note that these literature results were for uncentrifuged samples which almost certainly contained aggregates which probably sedimented out over time after the absorption measurement. An example of this is benzaldehyde. This is one of the best solvents for SWNTs presented by Detriche *et al.*[33] As part of this study, we tested benzaldehyde as a dispersant for SWNTs. Directly after sonication, benzaldehyde dispersions look very promising. However, over a period of days, the nanotubes tend to sediment out. When the samples are centrifuged, no nanotubes could be detected after centrifugation.

A better comparison would be with dispersion that has been centrifuged to remove all large aggregates, leaving only small bundles and individual SWNTs. As far as the authors are aware, the highest reported dispersibility for centrifuged solvent dispersions was 0.079 mg/mL for SWNTs dispersed in bromobenzene.[33] It is clear from Table 1 that 10 of our samples have dispersibilities above this value. Even solvent number 14, DMF, displays a dispersibility of 0.023 ± 0.006 mg/mL, not far below the bromobenzene result. In addition, after centrifugation, our samples are stable against aggregation and sedimentation over time scales of at least 1 month.

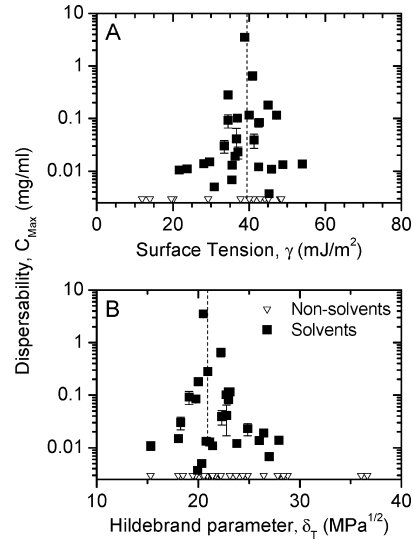

Figure 1. Maximum dispersibility, C_{max}, for both solvents and nonsolvents as a function of (A) solvent surface tension and (B) solvent Hildebrand parameter. Nonsolvents are those with dispersibilities of effectively zero. The vertical dashed lines illustrate the weighted mean of (A) the surface tension and (B) the Hildebrand parameter.

Surface Tension and Hildebrand Solubility Parameters. In our previous work, we showed that successful solvents tend to have surface energies very close to the surface energy of graphite.[17] This translates into surface tensions close to 40 mJ/m^2. As shown in Figure 1A, this is also the case in this work. However, while a useful guide for finding new solvents for nanotubes, surface tension is not a perfect solubility parameter. Some solvents, such as NMP, have almost perfect surface tension yet display significantly lower dispensability than CHP, which has very similar surface tension. In addition, many nonsolvents also have surface tensions close to 40 mJ/m^2 (Figure 1A). A more successful solubility parameter would address both of these issues.

As described above, the simplest general description of a good solvent is one whose Hildebrand parameter matches that of the solute.[21] To test this, we plot the measured nanotube dispersibility as a function of solvent Hildebrand parameter, as shown in Figure 1B. Here, the data clearly show a peak in the vicinity of $\delta_T = 21$ MPa$^{1/2}$. This is in good agreement with previous measurements of the Hildebrand parameters of SWNTs, double-walled nanotubes, and multiwalled nanotubes.[33] However, only a fraction of the solvents with the correct Hildebrand parameter will successfully disperse nanotubes. This has previously been attributed to the effects of surface entropy.[36] However, it is likely that the Hildebrand parameter is simply not specific enough to identify successful solvents. Thus, we need a more detailed set of solubility parameters. One possibility is the set of the Hansen solubility parameters.

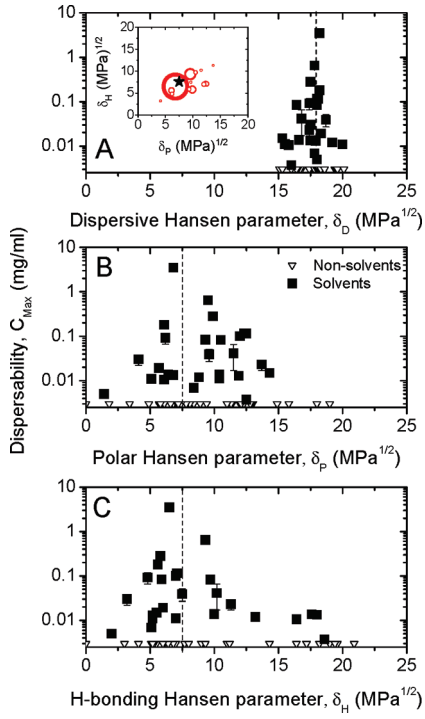

Figure 2. (A) Nanotube dispersibility as a function of the dispersive Hansen parameter, δ_D. The dashed line shows the position of the weighted average $<\delta_D>$. Inset: Plot of the H-bonding Hansen parameter, δ_H, *versus* the polar Hansen parameter, δ_P, of the solvents studied. For each solvent, the area of the data points is directly proportional to the nanotube dispersibility. The values $<\delta_H>$ and $<\delta_P>$ calculated for SWNTs are illustrated by the star. (B,C) Nanotube dispersibility as a function of the (B) polar Hansen parameter, δ_H, and (C) the H-bonding Hansen parameter, δ_H. The dashed lines show the position of the values $<\delta_H>$ and $<\delta_P>$ calculated for SWNTs.

Hansen Solubility Parameters. In order to estimate the Hansen parameters of the nanotubes, we plot the positions of the 14 most successful solvents in Hansen space, that is, using δ_D, δ_P, and δ_H as Cartesian coordinates (NB, these data are given in Table 1). These data are shown in Figure S1 in the Supporting Information, where the cross sectional area of each data point represents the relative dispersibility of the solvents used. It is immediately clear that all of the solvents lie within the same region of Hansen space.

In an attempt to make these data somewhat clearer, we plot the data for all solvents slightly differently in Figure 2. This graph shows the nanotube dispersibility as a function of the three Hansen parameters of the solvents used. Shown in Figure 2A, we see a sharp dependence on the dispersive Hansen parameter, with a peak close to 18 MPa$^{1/2}$. From this, successful solvents for nanotubes can be defined by $17 < \delta_D < 19$ MPa$^{1/2}$. This peak value of δ_D is close to the δ_D value measured for both SWNTs and double-walled nanotubes using the Hansen sphere method (19.4 and 18.5 MPa$^{1/2}$, respectively).[33] In addition, other studies have shown near-optimized SWNT dispersions to have δ_D values close to this.[34,37] Furthermore, carbon fibers have been reported to have $\delta_D = 21.3$ MPa$^{1/2}$.[38]

Shown in the inset of Figure 2A is a graph of the δ_P and δ_H values for the successful solvents. In this graph, the cross sectional areas of the data points are proportional to the SWNT dispersibility. These data are spread significantly in both the δ_H and δ_P directions. These data are also shown in Figure 2B,C as nanotube dispersibility as a function of δ_P and δ_H, respectively. In each case, a clear peak is observed close to the $\delta_P \approx 7.5$ MPa$^{1/2}$ and $\delta_H \approx 7.0$ MPa$^{1/2}$, respectively. From this, we can estimate that successful solvents for nanotubes are defined by $5 < \delta_P < 14$ MPa$^{1/2}$ and $3 < \delta_H < 11$ MPa$^{1/2}$. This agrees reasonably well with the data of Ham *et al.*[34] and Detriche *et al.*[33] In fact, the top four solvents for SWNTs reported by Detriche had $5 < \delta_P < 8$ MPa$^{1/2}$ and $3 < \delta_H < 5$ MPa$^{1/2}$, in good agreement with our results.

Hansen Parameters of Nanotubes. Solubility parameters of solutes can be found in a number of ways.[28] The simplest way is by solvent screening, that is, by associating the solubility parameters of the solute with those of the most successful solvents.[21,28,29,39] Often, the actual values for the three Hansen parameters of a solute are generally found from the Hansen parameter values for successful solvents using the Hansen sphere method (see ref 38 and references therein). In this method, "good" solvents are differentiated from "bad" solvents using predetermined criteria. The Hansen parameters of both good and bad solvents are plotted in Hansen parameter space. These data are then used to plot a sphere whose surface most effectively separates good solvents from bad solvents. The coordinates of the center of this sphere are then taken as the Hansen parameters of the solute. This method works well for systems where extensive data exist. However, it may not work so well for systems such as carbon nanotubes for which limited data exist. The problem here is that this method does not use any quantitative metric for the solvent quality and hence cannot differentiate good solvents from very good ones, for example.

We propose that a better method to estimate the Hansen parameters for solutes, where limited but quantitative data exist, is to calculate the weighted averages of the Hansen parameters of the successful solvents. We suggest using the quantitative measure of the solvent quality, here the dispersibility, as the weighting factor. Then the three Hansen parameters are given by

$$\langle \delta_i \rangle = \frac{\sum_{\text{solvent}} C_{\max} \delta_{i,\text{sol}}}{\sum_{\text{solvent}} C_{\max}} \qquad (11)$$

where i = D or P or H (or T). Here C_{max} is the dispersibility in a given solvent and $\delta_{i,sol}$ is the ith Hansen

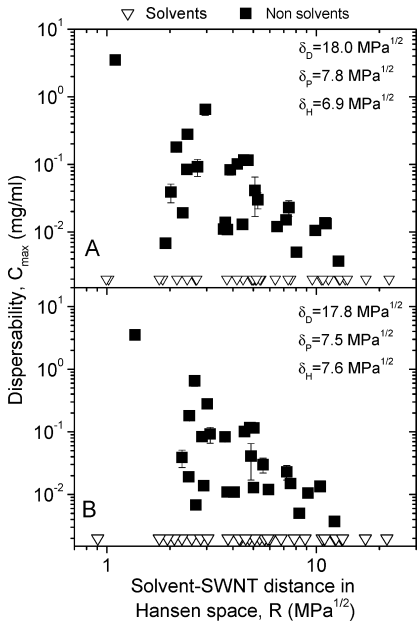

Figure 3. Nanotube dispersibility plotted as a function of solvent-SWNT distance in Hansen space for both solvents and nonsolvents. In A) the original set of nanotube Hansen parameters were used to calculate R, while in B) the refined set of SWNT Hansen parameters were used..

parameter in a given solvent. The summation is taken over all solvents studied. The advantage of this approach is that solvents contribute to the final result in proportion to their quality. We note that this procedure only works where one has observed a peak in the dispersibility as a function of each Hansen parameter.

For the solvents studied in this work, we estimate the Hansen parameters for nanotubes to be $<\delta_D> \approx 18.0$ MPa$^{1/2}$, $<\delta_P> \approx 7.8$ MPa$^{1/2}$, and $<\delta_H> \approx 6.9$ MPa$^{1/2}$. These values agree reasonably well with Detriche's Hansen sphere values, which were $\delta_D = 19.4$ MPa$^{1/2}$, $\delta_P = 6.0$ MPa$^{1/2}$, and $\delta_H = 4.5$ MPa$^{1/2}$ for SWNTs.[33] If the Hansen parameters for nanotubes presented here are correct, then solvents with Hansen parameters close to these should be good solvents. Moreover, nanotube dispersibility in a given solvent should decrease the further a solvent's Hansen parameters deviate from those of the nanotubes. This is just a manifestation of the fact that the dispersibility is expected to decrease as the enthalpy of mixing increases. We can test this by calculating the distance in Hansen space, R, from the point representing the solvent solubility parameters to that representing the nanotube solubility parameters. This is simply given by

$$R = \sqrt{(\delta_{D,A} - \delta_{D,B})^2 + (\delta_{P,A} - \delta_{P,B})^2 + (\delta_{H,A} - \delta_{H,B})^2} \quad (12)$$

If good solvents are those with all three Hansen parameters close to the nanotube Hansen parameters, then C_{max} should decrease as R increases. These data are plotted in Figure 3A and clearly show the expected trend, albeit with some scatter.

In order to improve our estimate of $<\delta_D>$, $<\delta_P>$, and $<\delta_H>$, we made the assumption that the correct values are those that give the C_{max} *versus* R graph with the least scatter. We wrote a MATLAB program to use inputted values of $<\delta_D>$, $<\delta_P>$, and $<\delta_H>$ to calculate R. The program then fit a straight line to a plot of log(C_{max}) *versus* log R and calculated the goodness of fit (taken as the square root of the sum of the square of the residuals). This was repeated for a grid of $<\delta_D>$, $<\delta_P>$, and $<\delta_H>$ in the vicinity of the values found from the weighted mean. We assume that the correct set of $<\delta_D>$, $<\delta_P>$, and $<\delta_H>$ is that which gives the best fit. We found the best fit for the values; $<\delta_D \geq 17.8$ MPa$^{1/2}$, $<\delta_P \geq 7.5$ MPa$^{1/2}$, and $<\delta_H \geq 7.6$ MPa$^{1/2}$. This refined set of Hansen parameters gave a slightly better straight line fit with R^2 increasing from 0.5 to 0.55.

Shown in Figure 3B is a graph of C_{max} *versus* R, where R is calculated using the refined set of nanotube Hansen parameters. In general, the scatter is slightly reduced compared to Figure 3A. These refined values for the nanotube Hansen parameters are likely to be more accurate than any others published because they are calculated after centrifugation for stable dispersions in extremely good solvents. We believe that these values will be useful to researchers in aiding solvent choice. We have included these values as the dashed lines in Figure 2 and the star in Figure 2A inset.

Nonsolvents. Also shown in Figure 3A,B are data for nonsolvents (*i.e.*, those where no nanotube material was reliably detected after centrifugation). These are indicated by arrows on the x axis. As we can also see from both panels A and B of Figure 3, there are a number of nonsolvents with very low R. According to standard solution theory, this should not be the case; solubility should be solely determined by R through its relationship with χ (for a given value of entropy of mixing which is small for SWNTs). We can illustrate this more clearly in Figure S2 in the Supporting Information. This is a map of the positions of solvents and nonsolvents in Hansen space. (We limit ourselves to solvents with $17 < \delta_D < 19$ MPa$^{1/2}$ and project the data onto the $\delta_H - \delta_D$ plane.) The Hansen parameters of SWNTs as calculated above are shown by the star. It is clear that both solvents and nonsolvents coexist in the vicinity of the star. It is not clear why some solvents in correct region of Hansen space do not disperse nanotubes. Detailed analysis has shown that this cannot be explained by nonsolvents having incorrect surface energies. A possible explanation is the presence of entropic effects due to solvent ordering at the nanotube surface.[36] However, it is also worth noting that our 14 most successful solvents all contain the amide structural unit: NC═O. We cannot rule out the presence of a specific interaction between such molecules and nanotubes. While other molecular types such as lactones[16] and amines[14] can disperse nanotubes relatively effectively, they have never demonstrated dispersibilities as

high as those reported here for the amide solvents. This points to the presence of a specific structural interaction.

In addition, we have plotted all of the solvents given in the HSPiP library with $17 < \delta_D < 19$ MPa$^{1/2}$ (www.hansen-solubility.com). It is clear from this that our analysis has only scratched the surface of the set of potential nanotube solvents. It would be interesting to map out more fully the distribution of solvents and nonsolvents in this region of Hansen space.

Fundamental Parameters. Finally, we reiterate that SWNTs are not small molecules. One significant difference between SWNTs and small molecules is that SWNTs have a well-defined surface. The solvent−nanotube interaction is localized at this surface. Thus, we might expect surface energies rather than cohesive energies to describe the interactions. In a previous paper, we used this point to derive an alternative version of eq 4, appropriate for cylindrical molecules with well-defined surfaces:[17]

$$\chi_s \approx \frac{2v_0}{R_{Bun}kT}(\partial_{T,NT} - \partial_{T,Sol})^2 \qquad (13)$$

Here, R_{Bun} is the radius of a SWNT and $\partial_{T,NT}$ and $\partial_{T,Sol}$ are the solubility parameters. In this case, the solubility parameters are related to the surface energy rather than the cohesive energy density: $\partial_T = \sqrt{E_{S,T}}$. This equation suggests that χ_S is minimized and so the dispersibility is maximized when the surface energy of the nanotube matches that of the solvent. Experiments have shown that to be the case for SWNTs (Figure 1A),[17] while equivalent results have also been demonstrated for solution exfoliated graphene.[40] This raises the question, which quantity, cohesive energy density, or surface energy is more fundamental for dispersions of nanostructured objects such as nanotubes, or indeed graphene?

We answer this question in two parts. Recently, Maiti *et al.*[32] and Usrey *et al.*[31] calculated Hildebrand solubility parameters for nanotubes using a number of methods. In each case, the solubility parameter was found to scale with nanotube diameter, *D*. These data, calculated using Maiti's method,[32] and by Usrey using the Fedors and refined solubility parameter (RSP) methods[41] have been reproduced in Figure 4A. It is clear that each method gives significantly different data for δ_T, ranging from 31 to 8.0 MPa$^{1/2}$ (in the diameter range appropriate for many SWNTs). The important point is that the cohesive energy density and so the solubility parameter is not intrinsic to nanotubes but scales with diameter. However, we can use the ideas on the role of surface expressed previously to derive an approximate expression for δ_T as a function of *D*.

The cohesive energy density of a nanotube crystal is approximately the energy required to separate all the individual nanotubes to infinity divided by the crystal volume. If there are *N* nanotubes in the crystal (where *N* is a large number to avoid edge effects), then the energy required to separate the nanotubes is $E_{NT} = N\pi DLE_{S,T}$, where *D* and *L* are the nanotube diameter and length and $E_{S,T}$ is the total nanotube surface energy. The volume of the crystal is just $V = N\pi D^2L/4$. This means the cohesive energy density is just $E_{C,T} = 4E_{S,T}/D$. Remembering that $\delta_T = \sqrt{E_{C,T}}$, we get

$$\delta_T = 2\sqrt{\frac{E_{S,T}}{D}} \qquad (14)$$

Previously, we estimated the surface energy to be 65−70 mJ/m^2,[17] a value supported by the data in Figure 1A. Using this value, we plot the Hildebrand parameter given by eq 14 on Figure 4A. It is clear from this plot that the diameter dependence embodied in Maiti's data is exactly reproduced by eq 14. In addition, we find that the values of δ_T generated by eq 14, using $E_{S,T} = 70$ mJ/m^2, lie in the middle of the calculated data. This result suggests that the nanotube solubility parameter is actually controlled by the nanotube surface energy, which is determined by the fundamental properties of the graphitic surface. This suggests that the Hansen parameters, while useful for identification of good solvents for nanotubes, are not fundamental quantities.

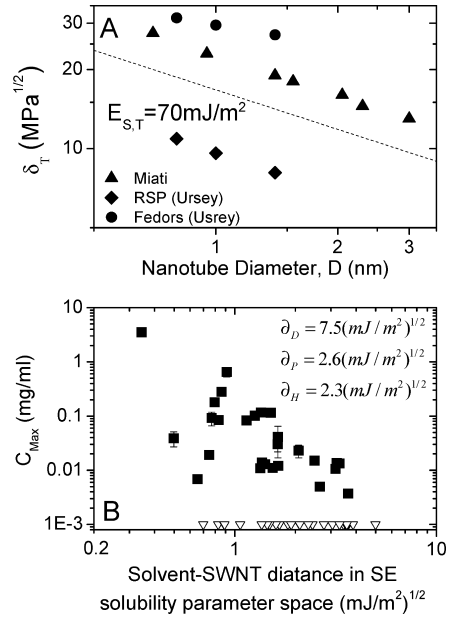

Figure 4. (A) Calculated Hildebrand parameter as a function of nanotube diameter (from Maiti *et al.* and Usrey *et al.*). The dashed line is a fit to eq 14 with surface energy; γ = 70 mJ/m^2. (B) Nanotube dispersibility plotted as a function of approximate surface energy Flory−Huggins parameter for solvents (solid squares) and nonsolvents (arrows on *x* axis).

Surface Energy Based Solubility Parameters. With this in mind, it would be advantageous to use Hansen-like solubility parameters, but related to the surface energy rather than the cohesive energy density. Such parameters would be related to the dispersive, polar, and hydrogen bonding components of the surface energy.

These components are available for a number of compounds but are not as readily accessible as Hansen parameters. It is well-known that the surface energy is related to the cohesive energy density (through the surface tension)[42,43] and so the Hildebrand parameter. Thus, we calculate these components from the Hansen parameters in a manner similar to that used by Beerbower[42] and Koenhen and Smolders.[43] Using this method, the ith component (i = D, P, or H) of the surface energy, $E_{S,i}$, is given by

$$E_{S,i} = \frac{\alpha_i \delta_i^2}{\alpha_D \delta_D^2 + \alpha_P \delta_P^2 + \alpha_H \delta_H^2} E_{S,T} \qquad (15)$$

where α_i are weighting factors for which various values have been proposed.[39,42,43] We find the best results are obtained using Beerbower's[42] values of α_i = 1 for i = D and α_i = 0.632 for i = P,H. In addition, we note that the surface energy is related to the surface tension, γ, by $E_{S,T} = \gamma + T\Delta S_S$.[44,45] Here ΔS_S is the solvent surface entropy which has the universal value of 0.1 mJ m^{-2} K^{-1} at room temperature.[44] By analogy with the discussion above, the associated solubility parameter components are found from $\partial_i = \sqrt{E_{S,i}}$ (i = D,P,H).

We have calculated the dispersive, polar, and H-bonding components of the surface energy and the associated solubility parameters for all of the solvents studied in this work. Unsurprisingly, when plotted against the surface energy solubility parameters, ∂_D, ∂_P, and ∂_H, the nanotube dispersibility displays peaks in all cases (Figure S3 in the Supporting Information). As before, we work out the surface energy solubility parameters of the nanotubes from the weighted means of the solvent surface energy solubility parameters. These are $\langle\partial_D\rangle$ = 7.5 (mJ/m^2)$^{1/2}$, $\langle\partial_P\rangle$ = 2.6 (mJ/m^2)$^{1/2}$, and $\langle\partial_H\rangle$ = 2.3 (mJ/m^2)$^{1/2}$. We note that our MATLAB routine was unable to improve on this estimate.

We can plot the dispersibility *versus* solvent−SWNT distance in SE solubility parameter space as shown in Figure 4B. As in Figure 3B, the nanotube dispersibility decreases reasonably smoothly with increasing R. This smooth decrease suggests that surface energy solubility parameter components can reasonably describe our data.

Finally, we note that there are a number of nonsolvents present in Figure 4B with low values of R. As mentioned above, this should not be the case as any successful solubility parameter should completely describe dispersibility. This shows that while the surface energy solubility parameters may have some advantages over Hansen parameters they do not provide the entire picture. As suggested above, it is entirely possible that specific structural interactions play some role in separating good solvents from nonsolvents.

The Role of Polar and H-Bonding Solubility Parameters. We note that it is perhaps surprising that polar and H-bonding solubility parameters play any role at all for systems such as carbon nanotubes. Their completely nonpolar nature would suggest that only the dispersion component should be important. However, the results presented here and elsewhere[33,34] show that correct values of δ_D (or ∂_D) are not enough. It remains unclear why this should be the case, although a number of possibilities exist. The presence of residual surface defects such as −OH or −COOH groups may impart nonzero δ_P and δ_H values on nanotubes. However, atomic resolution scanning tunneling microscopy measurements on HiPCO nanotubes have shown the defect content to be very low.[17] Thus, it is surprising that a very low defect content could have such influence. Alternatively, induced dipole effects may be important. This means it is possible that δ_P is actually an induction term while δ_H represents all other interactions. A similar partition has been proposed for the components of the surface energy.[39] In any case, the answer to this question remains out of reach at present. We leave it to others to solve this interesting problem.

Solubility of Nanotubes? The data and analysis discussed in this paper allow us to consider the issue of nanotube solubility. As shown by Figure 3, a number of solvents have solubility parameters very close to those of the nanotubes. This suggests that some solvent−nanotube mixtures may have small enough χ to be true solutions. Using eq 10 (with the refined Hansen parameters), we can estimate χ values for the solvents studies to vary from ~0.1 for CHP to ~8 for triethyleneglycol. Previously, we used light scattering to measure a slightly negative value of χ for SWNTs in NMP.[17] Using eq 10, we estimate $\chi \sim 0.9$ for nanotubes in NMP. One explanation of this discrepancy is the approximations associated with the geometric mean approximation as described above. However, it seems more likely that χ really is positive for all of the solvents studied in this work. We can infer this by reference to Flory's theory of rigid rods. Flory's rigid rod theory predicts that for *athermal solutions* of rigid rods (*i.e.*, when $\chi = 0$) a nematic phase starts to appear above a critical concentration $C^* \approx 8\rho D/L$,[24] where ρ is the nanotube density and D and L are their diameter and length, respectively. In addition, the phase diagram for rod solutions (see for example Figure 4.13 in ref 24), when plotted as χ *versus* rod concentration, shows the presence of the "Flory Chimney". In essence, this means that the nematic phases start to appear at concentrations close to C^* for all negative values of χ. We can estimate $C^* \sim 15$ mg/mL for nanotubes. Experiments on highly oxidized multiwalled nanotubes in water have shown that centrifugation removes the nematic phase, leaving the isotropic phase at concentration slightly above C^*.[46] This suggests that the maximum dispersibility for nanotubes with $\chi \leq 0$ would be ~15 mg/mL. However, the best result we obtained was 3.5 mg/mL in CHP. This strongly suggests that χ cannot be negative for any of the

nanotube−solvent mixtures studied in this work. In addition, Flory's phase diagram shows that, for χ above some well-defined positive value, the concentration above which the nematic phase starts to appear begins to decrease with increasing χ. Given that centrifugation removes the nematic phase, this would mean the measured dispersibility would decrease with increasing χ in this region. As this is what is observed here, this confirms that $\chi > 0$ for all of the solvent−nanotube mixtures studied.

This raises the question as to whether χ is small enough for any of the mixtures such that the entropic component of the free energy outweighs the enthalpy, so that we have a solution. Given the inaccuracies introduced into eq 10 by the geometric mean approximation for mixtures with low χ, this question cannot be answered by calculating $\Delta\tilde{H}_{mix}$ and $\Delta\tilde{S}_{mix}$ using eqs 3, 10, and 6. However, we note that all solvents studied, including CHP, tend to disperse nanotubes in the form of bundles.[16−18,47] In general, aggregates in solutions are generally limited in size to only a few molecules, typically <5.[48] While many bundles with <5 nanotubes are observed in CHP at all concentrations, significant populations of larger bundles are also found. For example, we have observed bundles with diameters up to ~5 nm in high concentration CHP dispersions. Such bundles contain ~25 nanotubes and should not exist in a true solution, suggesting that $\Delta\tilde{G}_{mix} > 0$, even for nanotubes in CHP. It remains unclear how to reconcile these data with our previous measurement of a negative χ in NMP. However, it is also hard to reconcile the presence of such bundles within the framework of aggregation theory. For insoluble solutes at concentrations above the critical aggregation threshold, the bundle size should be infinity (*i.e.*, all solute in a single aggregate). This is not observed in any of the (good) solvents studied. In addition, observations of these dispersions over the course of months have shown them to be very stable against aggregation; we do not observe the expected infinite aggregate forming. Thus, while we cannot conclude that nanotubes are soluble, the presence of 5 nm bundles is not compatible with them being insoluble in the normal sense. This may indicate that an additional effect, such as the charging suggested at the beginning of the paper, is responsible for their stabilization. Further work is required to definitively answer this question.

CONCLUSION

We have measured the dispersibility of SWNTs in a range of good solvents by measuring the concentration of nanotubes remaining after centrifugation. By plotting this dispersibility as a function of solvent Hansen solubility parameters, it is clear that successful solvents exist in only a small volume of Hansen space. The Hansen parameters of carbon nanotubes can be estimated by calculating the weighted average of the Hansen parameters of the successful solvents. Crucially, the nanotube dispersibility is used as the weighting factor. We propose that solubility parameters as derived from the cohesive energy density are not fundamental parameters for carbon nanotubes. To this end, we show that the diameter dependence of the Hildebrand parameter of nanotubes can be predicted from the nanotube surface energy. Furthermore, a new set of solubility parameters are suggested based on the surface energies of nanotubes and solvent. We suggest the surface energy to be the fundamental parameter determining the interaction of nanotubes with solvents.

In the absence of published tables of surface energy solubility parameters, Hansen parameters are probably the more practical set of solubility parameters for nanotubes. Indeed, these solubility parameters can be (and have been) used very successfully to aid solvent discovery. However, they unfortunately remain imperfect. A number of nonsolvents exist in the region of Hansen parameter space close to the solubility parameters of nanotubes. This is contrary to solubility theory and certainly limits the utility of this method. In the future, it will be critical to gain a fuller understanding of solvent−nanotube interactions to determine the distinction between solvents and nonsolvents.

METHODS

Dispersions of single-walled carbon nanotubes (SWNTs) (HiPCO, purchased from Unidym, www.unidym.com, lot number P0288) were prepared, as previously reported,[17,18] in a range of known organic solvents as follows: an initial SWNT concentration of either 5 or 1 mg/mL was subjected to 30 min of tip-sonication (VibraCellCVX, 750 W, 20%, 20 kHz), with ice-cooling, and allowed to stand for 24 h. In general, we used 1 mg/mL to avoid excessive nanotube loss on centrifugation, but for the systems with highest dispersibility, we used 5 mg/mL. For systems with dispersibility just below 1 mg/mL, we checked that both starting concentrations gave similar results. The solvents used were *N*-methyl-2-pyrrolidone (NMP), 1,3-dimethyl-2-imidazolidinone (DMEU), *N*-vinylpyrrolidone (NVP), *N*-dimethylacetamide (DMA), *N*-dimethylformamide (DMF), 1-cyclohexylpyrrolidone (CHP), *N*-butyl-2-pyrrolidone (NBuP), *N*-ethyl-2-pyrrolidone (NEP), 1-benzyl-2-pyrrolidinone (NBenP), dimethyltetrahydro-2-pyrimidinone (DMPU), oxo-pyrrolidine propionitrile (OPPN), *N*-octylpyrrolidone (N8P), *N*-dodecylpyrrolidone (N12P), and *N*-formylpiperidine (NFP). The simplified molecular input line entry specification codes (SMILES codes) and molecular structures for all these solvents are given in the Supporting Information, Table S2. All solvents were purchased from Sigma-Aldrich and used as received. Following sonication, large aggregates were removed from these dispersions with a mild centrifugation (CF) step (5500 rpm for 90 min; Hettich Mikro 22R), resulting in a supernatant composed of small SWNT bundles.[17,18] The concentration, C_{max}, of SWNTs remaining after CF was determined by measuring the dispersion absorbance (660 nm),[18] A (Cary 6000i, UV−vis−NIR). This was converted into the concentration using the Beer−Lambert law: $A = \alpha C_{max} l$ where l is the cell length and the extinction coefficient for SWNTs was taken as $\alpha = 3264$ mL mg^{-1} m^{-1}.[18] Dispersions

of each solvent were prepared six times and the concentration of SWNTs remaining after centrifugation was averaged. The error in concentration was taken as the standard deviation over the six absorbance measurements. The Hansen parameters of the solvents were either taken from the literature[29] or calculated using published algorithms[49,50] incorporated into HSPiP software (www.hansen-solubility.com; see Supporting Information).

Acknowledgment. We would like to thank Steve Abbott and Charles Hansen for useful discussions. J.N.C. acknowledgments SFI funding under the PI award scheme, contract number 07/IN.1/I1772.

Supporting Information Available: A description of the calculation of unknown Hansen parameters. A three-dimensional graph of the positions of the 14 best solvents in Hansen parameter space. Two-dimensional graph showing δ_P and δ_H values for solvents and nonsolvents. Graphs of nanotube dispersibility *versus* dispersive, polar, and H-bonding surface energy solubility parameters. Table showing solvents and nonsolvents. Detailed information on top 14 solvents. This material is available free of charge *via* the Internet at http://pubs.acs.org.

REFERENCES AND NOTES

1. Baughman, R. H.; Zakhidov, A. A.; de Heer, W. A. Carbon Nanotubes—The Route toward Applications. *Science* **2002**, *297*, 787–792.
2. Coleman, J. N.; Khan, U.; Blau, W. J.; Gun'ko, Y. K. Small but Strong: A Review of the Mechanical Properties of Carbon Nanotube−Polymer Composites. *Carbon* **2006**, *44*, 1624–1652.
3. Bachilo, S. M.; Strano, M. S.; Kittrell, C.; Hauge, R. H.; Smalley, R. E.; Weisman, R. B. Structure-Assigned Optical Spectra of Single-Walled Carbon Nanotubes. *Science* **2002**, *298*, 2361–2366.
4. Duesberg, G. S.; Burghard, M.; Muster, J.; Philipp, G.; Roth, S. Separation of Carbon Nanotubes by Size Exclusion Chromatography. *Chem. Commun.* **1998**, 435–436.
5. O'Connell, M. J.; Bachilo, S. M.; Huffman, C. B.; Moore, V. C.; Strano, M. S.; Haroz, E. H.; Rialon, K. L.; Boul, P. J.; Noon, W. H.; Kittrell, C.; Ma, J. P.; Hauge, R. H.; Weisman, R. B.; Smalley, R. E. Band Gap Fluorescence from Individual Single-Walled Carbon Nanotubes. *Science* **2002**, *297*, 593–596.
6. Coleman, J. N.; Ferreira, M. S. Geometric Constraints in the Growth of Nanotube-Templated Polymer Monolayers. *Appl. Phys. Lett.* **2004**, *84*, 798–800.
7. Murphy, R.; Coleman, J. N.; Cadek, M.; McCarthy, B.; Bent, M.; Drury, A.; Barklie, R. C.; Blau, W. J. High-Yield, Nondestructive Purification and Quantification Method for Multiwalled Carbon Nanotubes. *J. Phys. Chem. B* **2002**, *106*, 3087–3091.
8. Cathcart, H.; Nicolosi, V.; Hughes, J. M.; Blau, W. J.; Kelly, J. M.; Quinn, S. J.; Coleman, J. N. Ordered DNA Wrapping Switches on Luminescence in Single-Walled Nanotube Dispersions. *J. Am. Chem. Soc.* **2008**, *130*, 12734–12744.
9. Zheng, M.; Jagota, A.; Semke, E. D.; Diner, B. A.; McLean, R. S.; Lustig, S. R.; Richardson, R. E.; Tassi, N. G. DNA-Assisted Dispersion and Separation of Carbon Nanotubes. *Nat. Mater.* **2003**, *2*, 338–342.
10. Ausman, K. D.; Piner, R.; Lourie, O.; Ruoff, R. S.; Korobov, M. Organic Solvent Dispersions of Single-Walled Carbon Nanotubes: Toward Solutions of Pristine Nanotubes. *J. Phys. Chem. B* **2000**, *104*, 8911–8915.
11. Bahr, J. L.; Mickelson, E. T.; Bronikowski, M. J.; Smalley, R. E.; Tour, J. M. Dissolution of Small Diameter Single-Wall Carbon Nanotubes in Organic Solvents. *Chem. Commun.* **2001**, 193–194.
12. Furtado, C. A.; Kim, U. J.; Gutierrez, H. R.; Pan, L.; Dickey, E. C.; Eklund, P. C. Debundling and Dissolution of Single-Walled Carbon Nanotubes in Amide Solvents. *J. Am. Chem. Soc.* **2004**, *126*, 6095–6105.
13. Landi, B. J.; Ruf, H. J.; Worman, J. J.; Raffaelle, R. P. Effects of Alkyl Amide Solvents on the Dispersion of Single-Wall Carbon Nanotubes. *J. Phys. Chem. B* **2004**, *108*, 17089–17095.
14. Maeda, Y.; Kimura, S.; Hirashima, Y.; Kanda, M.; Lian, Y. F.; Wakahara, T.; Akasaka, T.; Hasegawa, T.; Tokumoto, H.; Shimizu, T.; Kataura, H.; Miyauchi, Y.; Maruyama, S.; Kobayashi, K.; Nagase, S. Dispersion of Single-Walled Carbon Nanotube Bundles in Nonaqueous Solution. *J. Phys. Chem. B* **2004**, *108*, 18395–18397.
15. Umek, P.; Vrbanic, D.; Remskar, M.; Mertelj, T.; Venturini, P.; Pejovnik, S.; Mihailovic, D. An Effective Surfactant-Free Isolation Procedure for Single-Wall Carbon Nanotubes. *Carbon* **2002**, *40*, 2581–2585.
16. Bergin, S. D.; Nicolosi, V.; Giordani, S.; de Gromard, A.; Carpenter, L.; Blau, W. J.; Coleman, J. N. Exfoliation in Ecstasy: Liquid Crystal Formation and Concentration-Dependent Debundling Observed for Single-Wall Nanotubes Dispersed in the Liquid Drug Gamma-Butyrolactone. *Nanotechnology* **2007**, *18*, 455705.
17. Bergin, S. D.; Nicolosi, V.; Streich, P. V.; Giordani, S.; Sun, Z.; Windle, A. H.; Ryan, P.; Peter, N.; Niraj, P.; Wang, Z.-T. T.; Carpenter, L.; Blau, W. J.; Boland, J. J.; Hamilton, J. P.; Coleman, J. N. Towards Solutions of Single-Walled Carbon Nanotubes in Common Solvents. *Adv. Mater.* **2008**, *20*, 1876–1881.
18. Giordani, S.; Bergin, S. D.; Nicolosi, V.; Lebedkin, S.; Kappes, M. M.; Blau, W. J.; Coleman, J. N. Debundling of Single-Walled Nanotubes by Dilution: Observation of Large Populations of Individual Nanotubes in Amide Solvent Dispersions. *J. Phys. Chem. B* **2006**, *110*, 15708–15718.
19. Cai, L. T.; Bahr, J. L.; Yao, Y. X.; Tour, J. M. Ozonation of Single-Walled Carbon Nanotubes and Their Assemblies on Rigid Self-Assembled Monolayers. *Chem. Mater.* **2002**, *14*, 4235–4241.
20. Ciferri, A. *Liquid Crystallinity in Polymers*; Wiley: New York, 1991; p 438.
21. Hildebrand, J. H.; Prausnitz, J. M.; Scott, R. L. *Regular and Related Solutions*, 1st ed.; Van Nostrand Reinhold Company: New York, 1970; p 228.
22. Rubinstein, M.; Colby, R. H. *Polymer Physics*, 1st ed.; Oxford University Press: Oxford, 2003; p 440.
23. Flory, P. J. *Principles of Polymer Chemistry*; Cornell University Press: Ithaca, NY, 1953.
24. Donald, A.; Windle, A. H.; Hanna, S. *Liquid Crystalline Polymers*; Cambridge University Press: Cambridge, 2006.
25. Torrens, F. Calculations on Solvents and Co-Solvents of Single-Wall Carbon Nanotubes: Cyclopyranoses. *J. Mol. Struct. (THEOCHEM)* **2005**, *757*, 183–191.
26. Sun, Z.; Nicolosi, V.; Rickard, D.; Bergin, S. D.; Aherne, D.; Coleman, J. N. Quantitative Evaluation of Surfactant-Stabilized Single-Walled Carbon Nanotubes: Dispersion Quality and Its Correlation with Zeta Potential. *J. Phys. Chem. C* **2008**, *112*, 10692–10699.
27. White, B.; Banerjee, S.; O'Brien, S.; Turro, N. J.; Herman, I. P. Zeta-Potential Measurements of Surfactant-Wrapped Individual Single-Walled Carbon Nanotubes. *J. Phys. Chem. C* **2007**, *111*, 13684–13690.
28. Brandrup, J.; Immergut, E. H.; Grulke, E. A.; Akihiro, A.; Bloch, D. R. *Polymer Handbook*, 4th ed.; Wiley & Sons: New York, 1999.
29. Hansen, C. M. *Hansen Solubility Parameters - A User's Handbook*; CRC Press: Boca Raton, FL, 2007.
30. Prigogine, I. *The Molecular Theory of Solutions*; North-Holland: Amsterdam, 1957.
31. Usrey, M. L.; Chaffee, A.; Jeng, E. S.; Strano, M. S. Application of Polymer Solubility Theory to Solution Phase Dispersion of Single-Walled Carbon Nanotubes. *J. Phys. Chem. C* **2009**, *113*, 9532–9540.
32. Maiti, A.; Wescott, J.; Kung, P. Nanotube−Polymer Composites: Insights from Flory−Huggins Theory and Mesoscale Simulations. *Mol. Simul.* **2005**, *31*, 143–149.
33. Detriche, S.; Zorzini, G.; Colomer, J. F.; Fonseca, A.; Nagy, J. B. Application of the Hansen Solubility Parameters Theory to Carbon Nanotubes. *J. Nanosci. Nanotechnol.* **2007**, *8*, 6082–6092.

34. Ham, H. T.; Choi, Y. S.; Chung, I. J. An Explanation of Dispersion States of Single-Walled Carbon Nanotubes in Solvents and Aqueous Surfactant Solutions Using Solubility Parameters. *J. Colloid Interface Sci.* **2005**, *286*, 216–223.
35. Yokoi, T.; Iwamatsu, S.; Komai, S.; Hattori, T.; Murata, S. Chemical Modification of Carbon Nanotubes with Organic Hydrazines. *Carbon* **2005**, *43*, 2869–2874.
36. Grujicic, M.; Cao, G.; Roy, W. N. Atomistic Simulations of the Solubilization of Single-Walled Carbon Nanotubes in Toluene. *J. Mater. Sci.* **2004**, *39*, 2315–2325.
37. Cheng, Q. H.; Debnath, S.; Gregan, E.; Byrne, H. J. Effect of Solvent Solubility Parameters on the Dispersion of Single-Walled Carbon Nanotubes. *J. Phys. Chem. C* **2008**, *112*, 20154–20158.
38. Launay, H.; Hansen, C. M.; Almdal, K. Hansen Solubility Parameters for a Carbon Fiber/Epoxy Composite. *Carbon* **2007**, *45*, 2859–2865.
39. Barton, A. F. M. *CRC Handbook of Solubility Parameters and Other Cohesion Parameters*; CRC Press: Boca Raton, FL, 1983.
40. Hernandez, Y.; Nicolosi, V.; Lotya, M.; Blighe, F. M.; Sun, Z. Y.; De, S.; McGovern, I. T.; Holland, B.; Byrne, M.; Gun'ko, Y. K.; Boland, J. J.; Niraj, P.; Duesberg, G.; Krishnamurthy, S.; Goodhue, R.; Hutchison, J.; Scardaci, V.; Ferrari, A. C.; Coleman, J. N. High-Yield Production of Graphene by Liquid-Phase Exfoliation of Graphite. *Nat. Nanotechnol.* **2008**, *3*, 563–568.
41. Van Krevelen, D. W. H. P. J. *Properties of Polymers*; Elsevier Scientific Publishing: New york, 1976.
42. Beerbower, A. Surface Free Energy: A New Relationship to Bulk Energies. *J. Colloid Interface Sci.* **1971**, *35*, 126–132.
43. Koenhen, D. M.; Smolders, C. A. The Determination of Solubility Parameters of Solvents and Polymers by Means of Correlations with Other Physical Quantities. *J. Appl. Polym. Sci.* **1975**, *19*, 1163–1179.
44. Lyklema, J. The Surface Tension of Pure Liquids—Thermodynamic Components and Corresponding States. *Colloids Surf., A* **1999**, *156*, 413–421.
45. Tsierkezos, N. G.; Filippou, A. C. Thermodynamic Investigation of *N,N*-Dimethylformamide/Toluene Binary Mixtures in the Temperature Range from 278.15 to 293.15 K. *J. Chem. Thermodyn.* **2006**, *38*, 952–961.
46. Zhang, S. J.; Kinloch, I. A.; Windle, A. H. Mesogenicity Drives Fractionation in Lyotropic Aqueous Suspensions of Multiwall Carbon Nanotubes. *Nano Lett.* **2006**, *6*, 568–572.
47. Bergin, S. D.; Sun, Z. ; Streich, P. V.; Hamilton, J.; Coleman, J. N. New Solvents for Nanotubes: Matching the Dispersability of Surfactants. *J. Phys. Chem. C.* Submitted for publication.
48. Israelachvili, J. *Intermolecular and Surface Forces*, 2nd ed.; Academic Press: New York, 1991.
49. Isu, Y.; Nagashima, U.; Aoyama, T.; Hosoya, H. Development of Neural Network Simulator for Structure−Activity Correlation of Molecules (Neco). Prediction of Endo/Exo Substitution of Norbornane Derivatives and of Carcinogenic Activity of Pahs from C-13-NMR Shifts. *J. Chem. Inf. Comput. Sci.* **1996**, *36*, 286–293.
50. Stefanis, E.; Panayiotou, C. Prediction of Hansen Solubility Parameters with a New Group-Contribution Method. *Int. J. Thermophys.* **2008**, *29*, 568–585.